Chapter 6

ASPECT DEPENDENCE OF THE OPTICAL CONTINUUM

A major criticism of the unified interpretation for radio quasars has been the analysis of the Bologna (B2) sample of quasars by de Ruiter *et al.* (1986). They showed that the R-distribution for this complete low-frequency sample differs significantly from that for the 3CR sample. They concluded that the unified scheme of Orr & Browne (1982) is not sustained, because in this scheme all complete samples of radio quasars selected at low frequencies are expected to have their constituents randomly oriented in the sky and therefore exhibit similar R-distributions.

The above inconsistency could, however, be understood if the quasar sample of de Ruiter *et al.* (1986) were biased in some manner. The aspect dependence of the optical continuum (Browne & Wright, 1985) is a potential source of such a bias. In this chapter, the possibility that the Bologna sample may be ridden with a selection effect due to the optical continuum being dependent on orientation is explored. The results appear to support this conjecture, thus not only undermining the criticisms of de Ruiter *et al.* (1986), but also provoking a deeper analysis of the phenomenon of optical aspect dependence. Further support for the idea comes from an analysis of the data on host galaxies of quasars. The possible causes of the phenomenon are then discussed, as also the implications.

6.1 The Bologna quasars—an inconsistency with the unified scheme?

In order to conduct statistical studies of extragalactic radio sources, it is important to have samples of objects that are not biased with regard to the orientation of their radio axes. Only then can phenomenologies for these objects be quantitatively tested, especially if they postulate an orientation dependence for some of the concerned properties. It is generally assumed that samples of objects selected by surveys conducted at low radio frequencies would be unbiased with respect to source orientation. For, one would then be picking up sources by their extended radio emission (of steep radio spectrum) which is not relativistically beamed (or nearly so, cf. chapter 4), rather than by the emission from the central component (of flat radio spectrum) that *is* possibly Doppler boosted. It is also implicit that the optical emission from the nucleus is not dependent on orientation, and therefore, even if all the objects in such a complete low frequency sample are not identified, the quasars that are, are taken to constitute an *unbiased* sample.

There *are*, of course, suggestions, albeit model dependent, that a fraction of the optical continuum from the nucleus of some active galactic nuclei might be synchrotron emission that is relativistically beamed, especially among BL Lacertids and OVV (optically violently variable) quasars (e.g., Wardle *et al.*, 1984). However, these objects are of flat/complex radio spectrum of the extreme sort, and are not expected to constitute more than a very small fraction of complete low frequency samples, which therefore are generally assumed to remain "unbiased". The 3CR sample was the first among such samples, and was the one used by Orr & Browne (1982) to assign a numerical value to the model parameter in their unified scheme.

6.1.1 The Bologna sample

The B2 sample of quasars has been obtained from the Bologna radio survey that was conducted at 408 MHz (over a limited area of ~ 0.14 steradians of sky) and has a limiting radio flux density of 0.25 Jy. Those radio sources from the survey that were identifiable with stellar objects on the Palomar (POSS) plates and showed an excess of ultraviolet continuum were classified as quasars (a total of 74; Fanti *et al.*, 1975). The only purported selection effect in the sample is against objects of redshifts larger than 2.5 (because the criterion of ultraviolet excess was used). Therefore, this sample is "unbiased" as per the description given in the previous subsection, and more, has a radio flux density limit that is fainter than the 3CR sample. It is thus a sample that is doubly important in the context of relativistic beaming models; the deductions that have been made on the basis of such models (and tested on the 3CR sample) can now, in principle, be verified on an independent and fainter sample.

From VLA images obtained at 5 GHz, de Ruiter *et al.* (1986) determined the form of the distribution of $R_{observed}$ for 59 of the 74 quasars in the B2 sample. They found that it did not fit the theoretical distribution based on random orientation of the radio sources (Orr & Browne, 1982); their values of $R_{observed}$ were systematically higher by a factor of about five. They therefore stated that their data do not support the unified scheme.

It is important to confirm the result of de Ruiter *et al.* (1986) for the whole B2 sample. A more complete R distribution is shown in Fig. 6.1 (and the derivation of the values of R in it is described later in section 6.4.1). Also shown in the figure is the distribution of R for the 3CR sample (Fig. 1(a) of Orr & Browne, 1982). The peak in this updated Bologna distribution occurs somewhere between 0.1 and 1, while that for the 3CR distribution occurs between ~0.03 and 0.1. A further difference from the 3CR distribution is the significant fraction of objects with a large ($\gtrsim$ 10) value for $R_{observed}$. Thus, the observed differences are in fact even larger than was suggested by de Ruiter *et al.* (1986) on the basis of their restricted sample of 54 Bologna quasars.

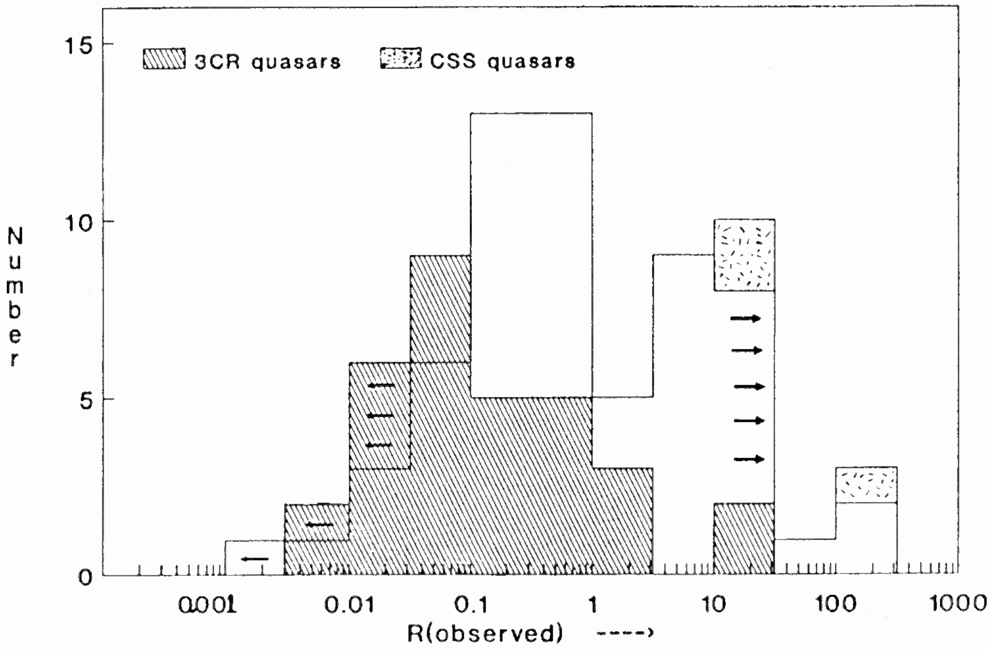

Fig.6.1 Distribution of $R_{observed}$ for B2 and 3CR quasars

For a majority of the quasars in the B2 sample, the redshifts are unknown. Hence, the values of R cannot be determined at the emitted frequency. Some of the disparity with the 3CR distribution could arise if the Bologna quasars have significantly higher redshifts. For, they would then be seen to larger emitted frequencies and hence the cores would appear more prominent intrinsically (due to the difference in spectral index between the cores (α typically ~ 0) and lobes (α typically ~ -1). The disparity, however, is too large to be explained by such an effect alone. Redshifts of about four would be required to explain a difference of a factor of five in the values of R.

It is thus important to examine if there are any selection effects in the B2 sample, and also if the proposition of Browne & Wright (1985) might explain the contrariety that de Ruiter *et al.* (1986) find with the scheme of Orr & Browne (1982).

6.1.2 Evidence for aspect dependence of the optical continuum

For sets of quasars of flat and steep radio spectrum from complete radio frequency samples, chosen such that these objects were *intrinsically similar* in the scheme of Orr & Browne (1982), a comparison of the apparent optical magnitude distributions has demonstrated that the distributions differ significantly (Browne & Wright, 1985). It may be noted that in unified schemes, a quasar with steep radio spectrum, if turned "end-on", would appear as one of flat radio spectrum *and* of higher radio flux density. Specifically, in the scheme of Orr & Browne, a typical lobe-dominated (steep radio spectrum) quasar (LDQ) of flux density 0.3 Jy at 408 MHz and a core-dominated (flat radio spectrum) quasar (CDQ) of flux density of 1 Jy at 5 GHz are intrinsically identical objects. Browne & Wright (1985) found that (radio-faint) LDQs appeared optically fainter than (radio-bright) CDQs. In order to reconcile this difference in the distributions of apparent magnitudes with the scheme of Orr & Browne (1982), it is necessary to invoke a dependence of the optical continuum on aspect in the same sense as that of the radio emission. Browne & Wright (1985) suggested relativistic beaming or inclination dependent obscuration of the optical continuum at small angles to the line of sight as possible explanations for such an aspect dependence. They estimated that, for consistency, the average brightness of the continuum should change by at least 1 magnitude with orientation.

Wills & Browne (1986) also suggested that the optical continuum was aspect dependent, on the basis of evidence for an inverse correlation between equivalent widths of nuclear O[III] and H_β emission lines and the dominance of the radio core, and also between linewidth and core dominance. Relativistic beaming or thermal emission by a physically thin and optically thick disc were put forth as possibilities. In the latter case too, the amount of radiation received would differ with inclination angle, and this dependence on orientation would also be in the same sense as that of the radio emission if the disc were perpendicular to the radio jet.

6.1.3 The B2 sample—not really unbiased?

For the Bologna quasars, optical identifications have been looked for only down to the limiting apparent magnitude of the POSS plates, which is ~ 21. Now, it is well known that the distribution of apparent optical magnitude of a sample of quasars is a function of its limiting radio flux density: the median of the distribution of apparent magnitudes gets fainter with decrease in the radio flux density limit of the sample (Bolton & Wall, 1970). This effect is particularly strong for quasars selected from low-frequency catalogues, as can be seen from Fig. 1 of Browne & Wright (1985). At the flux density limit of the Bologna sample of 0.25 Jy, the peak occurs close to the POSS plate limit, suggesting that many QSOs would be too faint to be included in the sample. Deep optical observations of a sample selected at 408 MHz and complete to 1 Jy (from, in fact, the Bologna survey) have shown directly that as many as 40% of all quasar identifications are with objects below the POSS plate limit (Allington-Smith *et al.*, 1982). The fraction could be even higher at the flux density limit of 0.25 Jy.

Now, if the optical continuum is also a function of orientation in the same sense as the nuclear radio emission, the sample will pick up many quasars that are, so to speak, "intrinsically below the plate limit", but that get included because of their favourable inclination which causes the optical emission (along with the radio emission) to appear enhanced. The resulting sample would then *not* be unbiased with respect to orientation of radio structure axes. It should be pointed out that the cut-off effect of the optical continuum would be much less important for the 3CR quasars, because at the higher radio flux density limit of this sample, the distribution of apparent magnitudes peaks well above the POSS plate limit, and almost all the sources in the 3CR sample have in any case been optically identified from deeper optical observations.

6.2 Search for aspect dependence—the B2 quasars

If an aspect-dependent optical continuum does indeed result in an orientation bias in the Bologna sample, it should be revealed in the distributions of apparent magnitudes, m_v, of quasars with large and small values of $R_{observed}$. High resolution images of the Bologna quasars, mostly available in Rogora *et al.* (1986; 1987) are used here to investigate this question.

6.2.1 The derivation of $R_{observed}$

Of the 74 Bologna quasars listed in Fanti *et al.* (1979), three (0900+294, 0923+295 and 1340+319) have been condemned as misidentifications, after VLA images at high resolution revealed a displacement of ~ 5 arcsec between the optical position and the radio source (Rogora *et al.* 1986; 1987). The remaining 71 quasars have been considered below. 1320+299, 1328+307 and 1419+315 have been imaged by the VLA before (this thesis, Chapter 3; Perley, 1982). It may be noted that in the case of 1320+299, the radio "component" associated with the QSO is almost certainly unrelated to the other components observed by Feretti *et al.* (1982) (cf. description of the source, this thesis, section 3.3). It is therefore taken to be an independent source. 1419+315 also is almost certainly a juxtaposition of two unrelated radio sources (this thesis, section 3.3); only the triple source associated with the QSO is considered here to be the quasar.

For the remaining 68 quasars, flux densities of the nuclear components used for the estimation of $R_{observed}$ have been taken from high resolution VLA imaging data available in Rogora *et al.* (1986; 1987). It turns out that in 6 cases, the resolution of the image or the accuracy of the optical position is insufficient to identify the nuclear component (although the identification of the radio source itself as a quasar is secure), and therefore the value of $R_{observed}$ cannot be determined. These objects have therefore to be excluded from the analysis. The flux densities of the extended emission have been taken from the VLA data of Rogora *et al.* whenever available. If the VLA images do not detect any extended emission, then the total flux densities measured at 5 GHz by Fanti *et al.* (1979) using the WSRT are used. In some cases, the radio flux density has clearly varied and the flux density of the unresolved component as given by the VLA image is higher than the total flux density as measured by the WSRT. In these cases, an approximate estimate of $R_{observed}$ is made using the radio spectral index of the radio source between 1.4 and 5 GHz (Fanti *et al.*, 1979), and assuming that the radio quasar consists of a nuclear component of spectral index 0 and extended emission of spectral index −1. Since for sources with inverted spectrum this estimate is invalid, a lower limit for the value of $R_{observed}$ is estimated from the $R_{observed}$ − α relation presented in Fig. 6.2. The relevant properties for the 71 Bologna quasars are presented in Table 6.1.

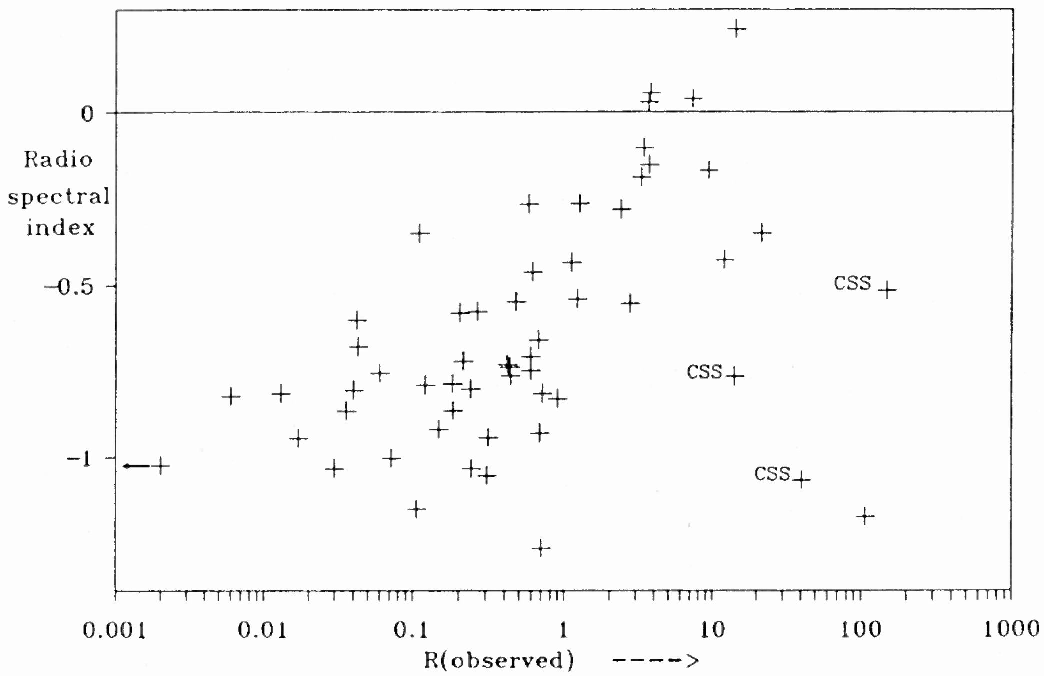

Fig. 6.2 Radio spectral index vs. $R_{observed}$ for B2 quasars

6.2.2 The B2 sample—not unbiased!

Fig. 6.3a and b show the distributions of apparent magnitudes for the two

Table 6.1 The quasars from the Bologna (B2) sample. The radio spectral index is estimated between 1.4 and 5 GHz.

Source	Apparent Optical Magnitude	Radio Spectral Index	R	Remarks
0808+289	18.8	-0.55	2.8	
0810+327	18.0	-0.10	3.4	
0816+268	18.2	-0.80	0.2	
0836+296	20.8	-0.68	0.04	
0853+291	19.1	-1.00	0.07	
0900+294		-1.15		Misidentified
0901+285	17.6	-0.26	1.3	
0906+306	18.3	-0.46	0.6	
0906+313	17.8	-0.43	1.1	
0907+280	19.5	-1.15	0.1	
0909+302	20.3	-0.76	14.2	CSS
0912+297	16.3	-0.19	3.3	
0917+294	19.7	-0.86	0.2	
0920+312	19.5	-0.95	0.02	
0920+313	18.2	-0.15	3.7	
0922+306	20.9	-1.06	0.3	
0922+316	20.0	0.04	7.3	
0923+295		-0.74		Misidentified
0928+312	18.6	-1.18	107	
0933+276	20.2	-1.03	0.03	
0937+304	18.2	-0.12	15.1	
0939+278	18.0	-0.94	0.3	
0953+307	20.2	-0.58	0.3	
0955+326	15.9	-0.43	12.0	
1002+281	20.6	-0.92	0.2	
1003+299	19.2	-0.72	0.2	
1003+328	19.0	-0.54	1.2	
1011+280	18.9	-0.27	0.6	
1015+277	19.1	-0.75	0.06	
1016+302	21.0	-0.60	0.04	
1017+318	20.3	-0.82	0.01	
1204+281	18.1	0.04	22.2	
1208+322	16.2	-0.93	0.7	
1211+284	20.0	-1.07	40.2	CSS
1213+307	19.2	-0.81	0.01	
1213+321	19.5	-0.35	21.4	

Table 6.1 (contd.)

Source	Apparent Optical Magnitude	Radio Spectral Index	R	Remarks
1215+303	15.1	-0.17	9.3	
1219+285	14.6	-0.34	3.8	
1222+320	18.1	-0.35	0.1	
1225+317	15.6	0.10	22.2	
1230+295	20.2	-0.74	0.4	
1234+268	20.5	-1.03	< 0.002	No core detected
1242+283	19.0	-1.27	0.7	
1244+324	18.2	-0.73	0.4	
1248+305	18.0	-0.87	0.04	
1254+285	20.9	-0.80	0.04	
1255+327	18.9	-0.01	156	
1308+326	19.5	0.17	22.2	
1320+299	20.7	-0.28	2.4	
1327+313	19.0	-1.09		Core position uncertain
1328+307	16.7	-0.51	148	CSS
1340+289	16.5	0.06	3.8	
1340+319		-0.76		Misidentified
1348+308	19.3	0.02	22.2	
1351+267	17.2	-0.83	0.9	
1351+318	17.4	-0.55	0.5	
1353+306	18.2	0.10	22.2	
1355+309	20.0	-0.98		Core position uncertain
1402+296	20.1	-0.79	0.1	
1410+317	20.5	-0.76	0.4	
1411+299	18.7	-0.75	0.6	
1419+315	20.0	-0.71	0.6	
1422+307	20.6	-1.03	0.2	
1425+267	15.4	-0.81	0.7	
1426+295	18.4	-0.63		Core position uncertain
1430+315	19.8	-0.87		Core position uncertain
1431+323	20.6	-0.58	0.2	
1435+315	18.0	0.03	3.7	
1443+266	18.8	-0.93		Core position uncertain
1448+301	19.5	-0.24		Core position uncertain
1451+270	19.7	0.24	14.3	
1452+301	19.0	-0.26	5.5	
1555+303	19.7	-0.66	0.7	
1620+301	19.4	-0.78	0.2	

subsamples of the Bologna quasars with $R_{observed} < 0.5$ and $R_{observed} > 0.5$ respectively. Of the quasars that appear compact with the A-array imaging by the VLA, 0909+130, 1211+284 and 1328+307 have steep radio spectra and are thus Compact Steep Spectrum (CSS) sources (cf., this thesis, section 4.3). To reiterate, CSS quasars do not fit in simply into the scheme of Orr & Browne (1982) and are probably a different physical class of object. They have been shown stippled in the distribution.

There is a clear difference in the distributions of apparent optical magnitudes for quasars with low and high values of $R_{observed}$ (which is significant at the 0.01 level as derived by a Kolmogorov-Smirnov two-sample test). While the number of quasars with weak cores ($R_{observed} < 0.5$) continues to increase to the plate limit ($m_p = 21$), the quasars with prominent cores ($R_{observed} > 0.5$) peak before the plate limit. The dependence of apparent optical magnitudes on the relative strength of the nuclear radio component is also evident from the plot of $R_{observed}$ versus m_p seen in Fig. 6.4. These parameters have been plotted for all the quasars in the sample except those for which the core identification (and therefore the $R_{observed}$ value) is uncertain. The two CSS sources have been marked separately. It is clear that there is a significant paucity of optically bright quasars with small values of R.

Indeed, it has been noted earlier that for the Bologna quasars, there is a dependence of the flattening of radio spectral index at high radio frequencies on the ratio of radio-to-optical flux density (Fanti *et al.*, 1975). Since the radio flux density used to calculate this ratio is that measured at 408 MHz where the nuclear component does not contribute significantly, this finding is roughly equivalent to the

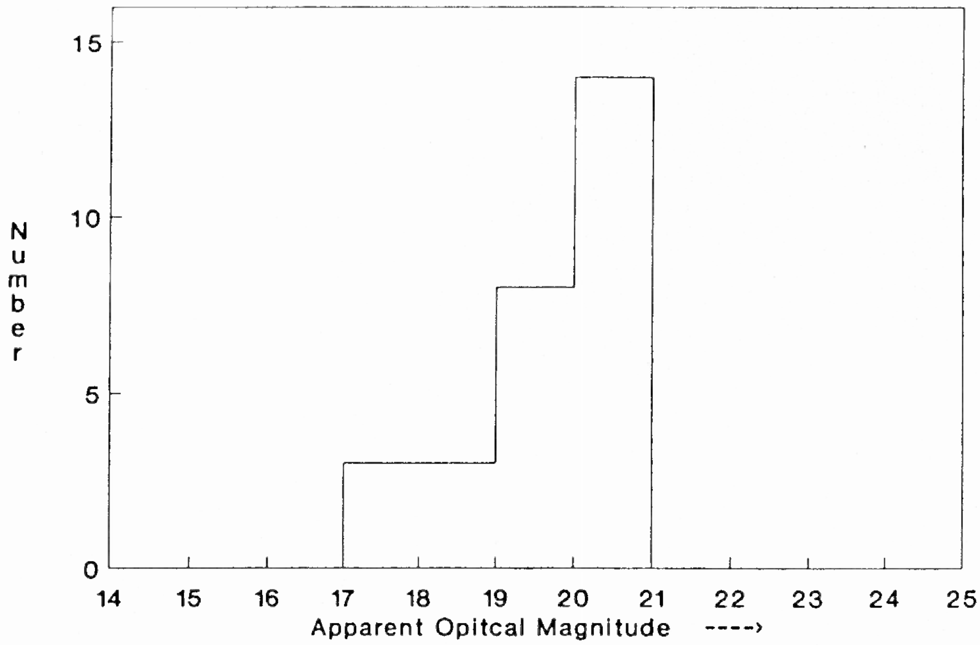

Fig.6.3a Distribution of optical magnitude: B2 quasars with R < 0.5

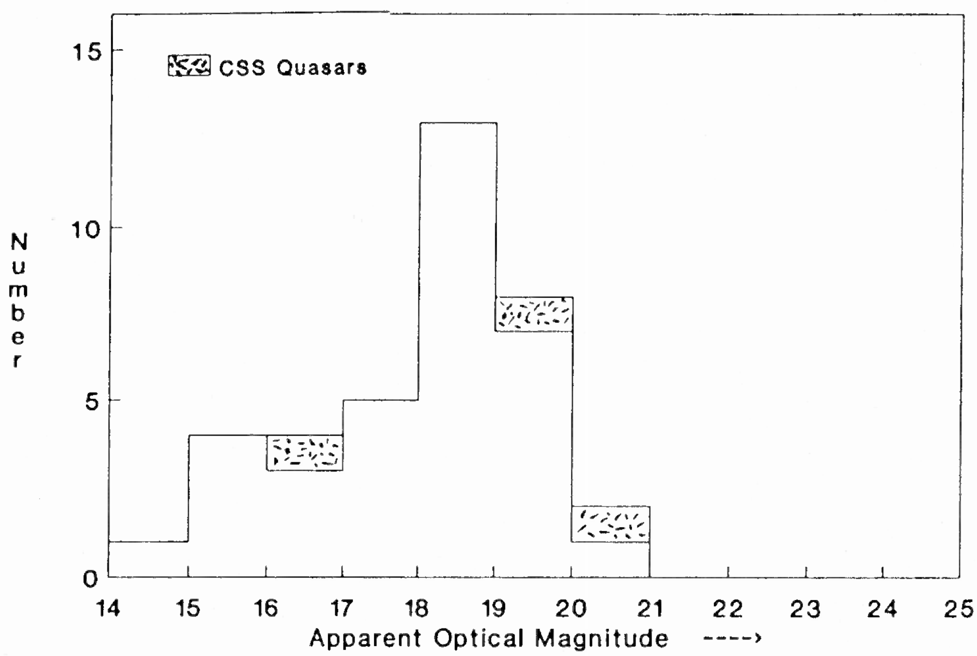

Fig.6.3b Distribution of optical magnitude: B2 quasars with R > 0.5

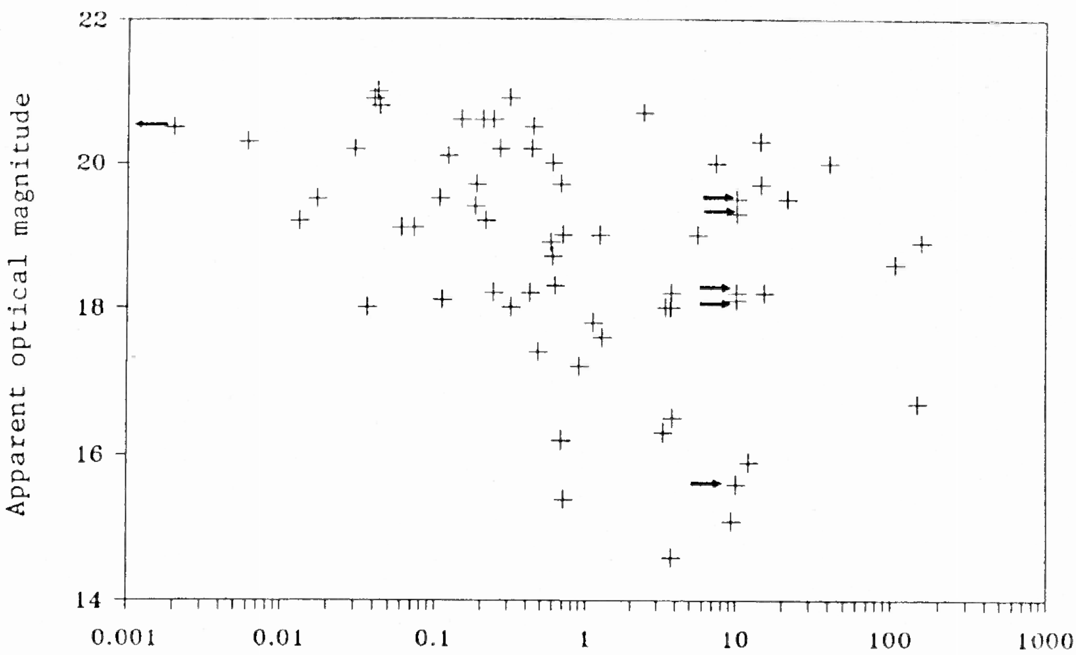

Fig. 6.4 Apparent optical magnitude vs. R_{obs} for B2 quasars

correlation between $R_{observed}$ and m_p described above.

It thus appears that the Bologna sample of quasars may be far from unbiased. A congruence of the distribution of $R_{observed}$ with what is predicted by the model of Orr & Browne (1982) can be expected, if at all, only when the optical identifications for the entire survey are *completed* and the optically fainter quasars thereby identified. The above arguments predict that these optically fainter objects would have relatively low values of $R_{observed}$.

6.3 Search for aspect dependence—other support for the R-m correlation

It turns out that the trend for flat radio spectrum (and therefore core-dominated) quasars to be optically brighter than their lobe-dominated counterparts has been noticed earlier, though the results were not interpreted as a manifestation of the orientation effect. These cases are briefly described below. The more recent evidence for the same phenomenon from the Molonglo sample is also summarized.

6.3.1 Earlier instances of the same phenomenon

Wills & Lynds (1978) found that quasars with flat radio spectrum were optically brighter than those with steep radio spectrum in their complete samples of quasars selected at 178 MHz, and also for the ones selected at 2.7 GHz (though to lesser level of significance). Condon *et al.* (1981) also pointed out that the Bologna quasars with steep and flat radio spectrum differed in their apparent magnitude distributions. The study of the Parkes sample of quasars selected at 2.7 GHz in the strip of sky of ± 4° declination by Masson & Wall (1977) is another investigation that showed a similar disparity in apparent magnitude distributions between quasars of flat and steep radio spectrum.

In view of the fact that quasars with flat radio spectrum, in addition to appearing optically brighter, also tend to have compact radio structures, Wills & Lynds (1978) put forth two alternative explanations: (a) that the same physical conditions (within the object or in its environment) that constrict the expansion of the radio source also brighten the optical continuum, or (b) that more compact objects were younger and therefore also optically more luminous. There are several CSS sources now known in whose case it is strongly suspected that a gas-rich interstellar medium constricts the size of the radio source through interactions (cf. section 4.3 and references therein). But in these cases the radio spectrum turns out to be steep and not flat, and it is not clear whether the interaction can occur close enough to the nucleus and thereby produce a brighter optical continuum. In any case, while hypothesis (a) would explain the correlation of R with apparent misalignments near the nucleus (Chapter 5), it does not explain the correlation of R with large scale misalignments (Kapahi & Saikia, 1982). As for alternative (b), while one might argue that the radio (and optical) nuclear components of younger objects would be more powerful emitters, the conjecture does not explain the the correlation of "nuclear scale" misalignments with R (Chapter 5), much less the correlation of large scale misalignments with R. Neither hypothesis explains the correlation of the apparent superluminal velocity of radio components near the nucleus with R (Browne, 1987).

Condon *et al.* (1981) attributed the similar trend that they found for the Bologna quasars to a correlation between nuclear radio and optical luminosities. The correlation of R with m does not rule out this interpretation. However, it might even be viewed as consistent with orientation effects. For, relativistic beaming of the radio emission results in a higher *observed* radio luminosity for the nucleus, *and*, as has been argued earlier, is *accompanied* by an apparent enhancement of the optical luminosity as well. In any case, this interpretation points to the importance of determining the redshifts for all the B2 quasars. This will not only eliminate the uncertainties in R due to the unknown redshift but also enable testing of the correlation of radio and optical luminosities.

6.3.2 The Molonglo sample of quasars

Motivated by the prediction that unidentified (and therefore optically faint) quasars in complete low frequency samples will turn out to have large R, Kapahi *et al.* (1989) recently determined R values for a sample of radio-faint quasars from the

Molonglo Reference Catalogue of Large et al. (1981). The sample has a radio flux density limit of 0.95 Jy at 408 MHz and optical identifications have been made to a limiting magnitude of ~ 23, with all stellar objects taken to be quasars. Kapahi *et al.* (1989) have shown that the distributions of R for optically brighter (m_b < 19.5) and fainter ($m_b \geq 19.5$) objects differ from that for the 3CR quasars in that (a) sources with R > 10 appear to be more common, particularly in the optically brighter group, and (b) the peak of the R-distribution for the brighter quasars appears to occur at a larger value of R compared to that for the 3CR sample, while the opposite was true for the fainter quasars.

6.4 Search for optical aspect dependence—host galaxies of quasars

Much progress has been made in the investigation of the local environs of quasars since the early work of Kristian (1973) that detected a "fuzz" around several of them. The advent of charge-coupled device (CCD) detectors, which are of dramatically higher efficacy than the earlier photographic imagery, have hastened this process. It is now well established that the fuzz represents the host galaxy which the quasar inhabits. These hosts are larger and more luminous (massive?) than normal elliptical and spiral galaxies, with peculiar morphologies in several to boot. But of course, these differences from ordinary galaxies are not unexpected, since the presence of a violent energy source at the centre is bound to have its effect on the host. It is also possible that the peculiarities are causal, in that these are galaxies preferentially conducive to ultra–energetic central activity.

It also appears that radio loud quasars sit in giant elliptical hosts (Malkan, 1984; Gehren *et al.*, 1984; Smith *et al.*, 1986), which parallels radio galaxies being elliptical ones. (But it is not quite so clear if, correspondingly, radio–quiet quasars always occur in spiral hosts.)

6.4.1 Relativistic beaming and the L_{nucl}/L_{gxy} ratio

If (as in the unified scheme) differences among CDQs and LDQs are only due to orientation effects, it is expected that the luminosities of their host galaxies would similar. Hence, if the optical continuum from the active galactic nucleus is dependent on inclination, then the two groups of quasar should differ in their distributions of L_{nucl}/L_{gxy}, which is the ratio of optical emission from the nucleus to that from the host galaxy. This question has been explored in what follows, with an analysis of data from radio quasar images in the optical band available in the literature.

6.4.2 The correlation of L_{nucl}/L_{gxy} with $R_{observed}$

Hutchings *et al.* (1984) have presented photographic optical images (resolution of ~ 1 arcsec) of 78 quasars with redshifts of up to 0.7. Of these, 28 are radio-loud quasars, a set of reasonable size to look for systematic trends. The values of L_{nucl}/L_{gxy} are presented in table 1 of their paper. They decomposed the quasar images into the nuclear and host-galaxy components by subtracting a correctly scaled point-spread-function from the images so as to achieve the best exponential to the profile of the luminosity of the resolved part, averaged over azimuth. The values have been corrected for distance effects of the unresolved luminosity, for the dependence of the ratio on the point-spread-function and the limiting surface brightness of the image, for K–dimming, and for foreground extinction due to our Galaxy. Three of the quasars appear unresolved in the optical imaging.

For most of these objects, radio flux densities of the nucleus at 5 GHz using the VLA are available in Gower & Hutchings (1985), Perley (1982) and Harris *et al.* (1983). The value of $R_{observed}$ has thereby been derived. Wherever $R_{observed}$ cannot be determined reliably, the high frequency radio spectral index $\alpha^{\sim 1 \text{ to } 3GHz}_{\sim 5 \text{ to } 8GHz}$ has been used to estimate it as done in section 6.2.1.

Of the 28 radio loud quasars, 25 appear resolved (or marginally so) in the R band images and have values/upper limits of L_{nucl}/L_{gxy} tabulated. Of the three that appear unresolved, Gehren *et al.* (1984) have given upper limits for the absolute magnitudes (of the host galaxies) of two (0607–157 and 1203+011), from which approximate upper limits to L_{nucl}/L_{gxy} have been inferred. For 0742+318, an upper limit of ~ 30 has been assumed for the value of L_{nucl}/L_{gxy}. Table 6.2 lists these ratios.

Fig. 6.5 shows the plot of $R_{observed}$ against L_{nucl}/L_{gxy}. A distinct trend for objects with higher $R_{observed}$ to have higher values of L_{nucl}/L_{gxy}. Indeed, the trend is what the unified scheme would predict, because while enhancement of the radio emission from the core component is expected to be accompanied by enhancement of the optical continuum from the nucleus, no such change is expected of the emission from the host galaxy.

Table 6.2 Values of R and L_{nucl}/L_{gxy}

Source	Redshift	R_{obsd}	L_{nucl}/L_{gxy}
0007+106	0.09	2.4	2.6
0241+622	0.04	30	8.4
0607-157	0.32	0.6	> 33.0
0742+318	0.46	2.0	> 30.0
0752+258	0.45	3.9	7.0
0846+100	0.37	0.04	5.5
0851+202	0.31	7.3	> 23.0
0957+227	0.10	< 0.01	3.2
1011-282	0.25	0.2	13.0
1020-103	0.20	5.5	23.0
1203+011	0.10	> 10	> 5.9
1254-333	0.19	< 0.03	1.5
1302-102	0.29	8.8	4.7
1400+162	0.24	0.5	3.7
1425+267	0.37	0.7	1.0
1510-089	0.36	66	11.2
1525+227	0.25	0.4	6.4
1641+399	0.60	258	39.0
1704+608	0.37	0.3	4.0
1725+044	0.29	1.4	2.0
2135-147	0.20	0.1	3.7
2141+175	0.21	1.3	4.6
2201+315	0.30	1.9	3.3
2217+08N	0.62	0.9	0.1
2217+08S	0.22	0.1	0.2
2247+140	0.24	1.4	3.0
2305+187	0.31	0.2	0.2
2318+049	0.63	3.0	5.8

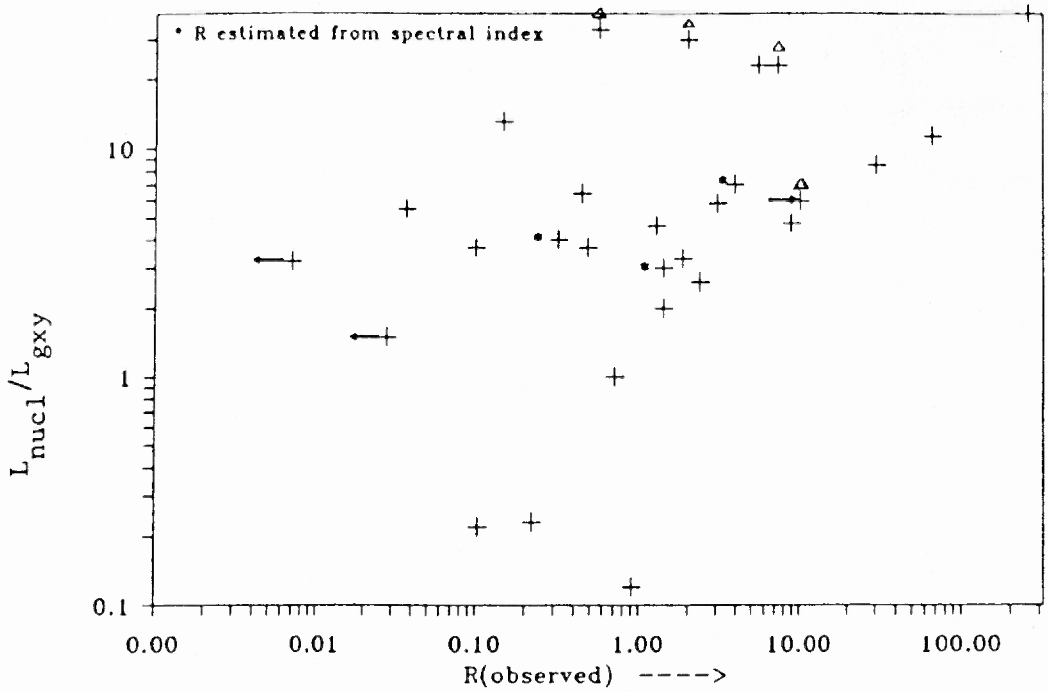

Fig. 6.5 L_{nucl}/L_{gxy} vs. R_{obs}

6.4.3 A caveat

It is important to point out here that there is some evidence that the host galaxies of quasars with steep radio spectrum emit O[III] lines of higher equivalent width than do the hosts of quasars with flat radio spectrum. Boroson & Oke (1984) found this on comparing data for three radio-loud quasars of flat radio spectrum with five of steep radio spectrum. Boroson *et al.* (1985) claim an analogous result. Among 10 radio-loud quasars in their list, four out of five with steep radio spectrum have large equivalent widths (i.e., > 23Å) of the O[III] emission line from the host galaxy, while only two out of five of those with flat radio spectrum do so. Stockton & MacKenty (1987) imaged several quasars in the narrow (30 Å) O[III] band, and detected extended O[III] emission from the host galaxy in 10 out of 26 quasars with steep radio spectrum, but only in 1 out of 7 quasars with flat radio spectrum.

The O[III] emission line would be redshifted into the R pass-band for $0.25 \lesssim z \lesssim 0.5$. Therefore, if host galaxies of flat radio spectrum are indeed under-luminous in O[III] emission, then the correlation of L_{nucl}/L_{gxy} with R could be a consequence of the smaller amount of radiation from the host galaxy in CDQs, rather than due to a relatively more luminous nucleus. More importantly, the fact that the host galaxies of quasars with small and large values of $R_{observed}$ may differ in the amounts of line emission that they radiate *would be a severe embarrassment to the unified scheme*, because it means that they are *intrinsically* different kinds of object. It is therefore very important to investigate this result with more systematic observations.

Along these lines, Smith *et al.* (1986) attempted an extensive study of the quasar host galaxies by putting together data from several optical imaging studies and their own. Assuming that data from different observing programmes can be combined if obtained through linear (rather than photographic) detectors (e.g., Gehren *et al.*, 1984) , they have confined their analysis to observations that have used linear detectors (CCD or SIT Vidicon). They obtain a sample of 86 quasars and their host galaxies, including 37 radio-loud quasars. But, in deriving the absolute magnitudes of the host galaxies in the sample, they correct for possible O[III] emission (on the basis of the result of Boroson *et al.* (1985) and using average values from the latter) for the categories of steep radio spectrum, flat radio spectrum, and radio-quiet quasars. While it is not clear that this is the correct procedure to adopt (since the number of objects in the Boroson *et al.* (1985) study is meagre), the corrected values do not show a significant correlation with radio spectral index.

Since CDQs of apparent radio luminosity comparable to LDQs are intrinsically much less luminous than the latter (cf. section 6.1.2), if one wishes to compare an aspect-independent parameter with a view to confront the unified scheme, then one must chose for the comparison CDQs and LDQs that are *predicted to be intrinsically similar* by the scheme. The observed correlation of O[III] luminosity with radio spectrum may, for example, be simply because more (intrinsically) radio luminous objects are more "O[III] luminous". Further, CSS quasars should be excluded from the comparison, because the unified interpretation does not apply to them. Clearly, the question has to be investigated carefully.

6.4.4 Beaming in optically/x–ray selected quasars—some speculations

Hutchings & Gower (1985) have used the behaviour of the L_{nucl}/L_{gxy} parameter to draw inferences about relativistic beaming in quasars. They have observed 41 of the optically/x–ray selected quasars from the sample of Hutchings *et al.* (1984) at 5 GHz with the VLA A-array. Those that they detect up to a limiting flux density of $\lesssim$ 1 mJy are of markedly higher optical luminosities and L_{nucl}/L_{gxy} values than those that they do not. They conclude that these findings are consistent with the optical and radio nuclear emission being Doppler beamed. They then state that "the luminous, often large, classical [radio-loud quasars] are probably more nearly isotropic emitters".

However, this does not really follow from the correlation of radio flux density with L_{nucl}/L_{gxy} for the non-radio-loud quasars. The correlation may be understood in the framework of the following unified phenomenology. There are broadly two populations of quasars (e.g., Peacock *et al.*, 1986.): the first consisting of radio-powerful CDQs and LDQs (that reside in elliptical hosts), and the second consisting of radio–quiet quasars (that probably reside in spiral hosts). In the case of the first population, the nuclear emission is relativistically beamed, and the CDQs are the objects oriented close to the line of sight, while LDQs are oriented close to the plane of the sky.

The radio-quiet quasars have their *total* radio emission relativistically beamed. The apparently stronger radio sources are thus close to the line of sight, and the really "radio-silent" ones (e.g., Kellermann *et al.*, 1986) are close to the plane of the sky. In other words, a relativistic beaming model akin to that of Scheuer & Readhead (1979) would apply. Indeed, the numbers of these sources increase with decreasing radio flux density in a manner that is roughly consistent with this model (Kellermann *et al.*, 1986). Thus, the extended radio structures in radio-quiet quasars are probably intrinsically small, and are intrinsically weaker versions of those seen in the radio–loud population. It is plausible that the Lorentz factors in the central components of radio-quiet quasars do not differ very significantly from those in their extensions (which are of the size of only a few kiloparsecs), because they are very close to the central component and have not decelerated significantly. The unified scheme of Orr & Browne (1982) would then not apply, because in this scheme, it is assumed that bulk relativistic motion occurs to a far higher degree in the nucleus than in the extensions. If the (relativistic) speeds are similar in the nuclear and outer components, then the parameter R would no longer be a measure of the angle of inclination to the line of sight. It is then no surprise that Kellermann *et al.* (1986) do not find a correlation of fraction of the radio core with total radio flux density S, for their sample (of quasars of the second population) with S < 100 mJy.

The curvatures observed by Gower & Hutchings (1985) in the extended radio structures, as well as their apparent one–sidedness might well be a consequence of small inclination angles and beaming effects. However, it is probably not meaningful to compare the observed projected linear sizes of optically detected QSOs with those of the radio–powerful quasars within single beaming model, since the difference in sizes is likely to be intrinsic.

6.5 Large-scale bulk relativistic motion and the optical continuum

So far in this chapter, the discussion on bulk relativistic motion has been confined to regions near the nucleus. However, evidence was presented in Chapter 4 in support of the conjecture that the radio emitting effluents continue to move at speeds that are mildly relativistic out to lengths of a few hundred kiloparsecs. This question of large-scale bulk relativistic motion in relation to the behaviour of the optical continuum from the nucleus (which appears to exhibit anisotropic characteristics as discussed in the previous pages) is considered in this section.

6.5.1 Quasars with detected jets—are they optically brighter?

If there is bulk relativistic motion on a large scale in quasars, then large-scale jets that are pointed towards the observer would have their flux density Doppler boosted, and would thereby be more easily detectable than those jets that are directed closer to the plane of the sky. This question was discussed in relation to other parameters of the radio structure that depend on orientation to the line of sight by Saikia (1984b). It was shown there that radio jets occur more frequently in quasars with relatively larger values of R. This was taken to suggest that the detected jets are generally directed at relatively small angles to the line of sight. Since it appears that the optical continuum is also apparently enhanced when the axis of the radio structure is inclined close to the line of sight (section 6.1), it is natural to ask if large-scale jets are more easily detectable in apparently brighter quasars. This has been done for a sample of well-imaged quasars, and is described in the following subsections.

6.5.2 Description of the sample

To decide if a quasar shows a detectable jet at the sensitivity limits of a given radio image, it is important to have an image of adequate resolution that delineates the elongated jet feature from the nuclear component and the extended lobes. In attempting to compile a sample rigorously, one encounters the expected problem: complete samples of radio quasars, with all the objects imaged with adequate resolution to a uniform sensitivity limit at radio wavelengths, are not available. Therefore, the question has been asked here for the best available eclectic set. A significant number of the radio images of quasars presented in Chapter 3 are adequate for the present purpose. To these have been added data on quasars from the literature for which radio images of the required resolution are available.

The selection criteria that were applied while choosing the sample are as follows. To have the sample homogeneous to the extent of being defined to a uniform radio flux density limit, the list has been confined to objects with radio flux density at 178MHz > 2Jy. As is customary, narrow elongated structures that are approximately three times longer than they are wide, and pointing to the nucleus at the point closest to it are regarded as jets. The compilation is confined to radio images with at least 10 synthesized beam elements across the elongation of the source so as to have sufficient resolution to delineate a jet structure. Most of the images have been made with the VLA.

The sample has a total of 88 objects; they are listed in Table 6.3, which is arranged as follows. Column 1 lists the name of the quasar. Column 2 indicates whether or not the radio image shows a jet. 'Possibly' in this column indicates that although an elongated structure that is actually three times longer than its width is not manifest, the image suggests that the source is very likely to show a jet at higher angular resolutions. The subsequent columns in the table list the redshift, the apparent V magnitude (as given by Hewitt & Burbidge, 1987), and a code of reference to the radio image. The codes and the corresponding references are listed in Table 6.4.

6.5.3 The distributions of apparent optical magnitudes

The sample has been split into objects that have detected jets and those that have not. The distributions of apparent optical magnitudes for the two categories are shown in Figs 6.6a and b. The distributions show that there is a considerably larger number of optically brighter objects among the quasars with detected large-scale radio jets, than among those which show no jets. This trend is to be expected if, on the one hand, enhancement of the observed optical continuum accompanies bulk

Table 6.3 Detectability of jets and optical magnitudes

Source	Jet detected?	Redshift	Optical Magnitude	Reference
0017+257	possibly	0.284	15.4	HUO
0017+154	YES	2.012	18.2	SSS
0041+119		0.228	19.0	HUO
0109+176	YES	2.157	18.0	Bar
0115+027	YES	0.672	17.5	present
0118+034		0.765	18.1	HUO;SSH
0133+207		0.425	18.1	SSH
0137+012	possibly	0.260	17.1	HUO
0225-014	possibly	2.037	18.2	Bar
0229+341		1.238	19.0	SSH
0312-034		1.072	18.3	SSH
0353+123	possibly	1.616	19.3	Bar
0404+177		1.712	19.2	Bar
0405-123	YES	0.574	14.8	RR
0723+679	YES	0.846	18.0	OP
0726+431		1.072	18.5	HUO
0730+257		2.686	20.0	Bar
0742+318	YES	0.462	16.0	NB
0802+103	YES	1.956	18.4	Bar
0805+046	possibly	2.877	18.2	Bar
0805+578		0.438	19.0	HUO
0812+020	YES	0.402	17.1	Wyck
0835+580		1.534	17.6	SSH
0836+195		1.691	17.6	Bar
0903+169	YES	0.411	18.3	SSH;HUO
0919+218	YES	1.421	18.5	present
0922+149		0.896	18.0	SSH
0926+117		1.754	19.1	Bar
0932+022		0.659	17.4	present;SSH
0957+003	YES	0.907	17.6	HUO;SSH
1004+130	YES	0.241	15.2	F81;MH
1007+417	YES	0.613	16.5	present;OP
1012+232	possibly	0.565	17.5	present
1012+488		0.385	19.0	HUO
1023+067		1.699	18.5	Bar
1040+123	YES	1.029	17.3	present
1100+772	YES	0.311	15.7	SSH;LM
1103-006	possibly	0.426	16.5	HUO
1104+167	YES	0.634	15.7	HUO
1111+408		0.734	18.0	SKN

Table 6.3 (contd.)

Source	Jet detected?	Redshift	Optical Magnitude	Reference
1118+128		0.685	18.0	HUO
1132+303	possibly	0.614	18.2	present
1136-135		0.557	16.1	present
1137+660		0.646	16.3	SSH
1150+497	YES	0.334	16.1	OP
1206+439		1.400	18.4	SKN;LM
1218+339	possibly	1.519	18.6	SBC
1221+186		1.401	18.7	SSH
1222+216	YES	0.435	17.5	present;HUO
1241+166	YES	0.557	19.0	SBC
1244+324	possibly	0.949	17.2	SSH
1248+305		1.061	17.5	SSH
1253-055	YES	0.538	17.8	dPP
1258+404	YES	1.659	19.4	SSS
1305+069		0.602	17.0	SSH
1308+182	YES	1.677	17.5	Bar
1317+520	YES	1.060	17.0	HUO;OP
1323+655		1.618	17.8	Bar
1345+584	YES	2.039	17.5	Bar
1354+195	YES	0.720	16.0	present;RR
1433+177	YES	1.203	18.2	present
1509+158	YES	0.828	18.2	present
1510-089	YES	0.361	16.5	OBC
1540+180	YES	1.662	18.0	Bar
1545+210		0.264	16.7	SSH
1548+114	YES	0.436	17.2	HUO
1602-001		1.625	17.5	Bar
1606+289		1.989	19.0	SSH
1618+177	YES	0.555	16.4	HUO
1620+356		1.473	18.5	HUO
1622+238		0.927	17.5	SSH
1623+173		0.552	19.0	HUO
1628+363	possibly	1.254	17.0	HUO
1704+608		0.371	15.3	SSH
1732+160		1.880	18.4	Bar
1739+184		0.186	16.4	SSH;HUO
1741+279	YES	0.372	17.7	present
1816+475	YES	2.225	18.2	Bar
1819+228		0.628	18.0	HUO
1830+285	possibly	0.594	17.2	HUO

Table 6.3 (contd.)

Source	Jet detected?	Redshift	Optical Magnitude	Reference
1857+566	YES	1.595	17.3	S83;Bar
1928+738	possibly	0.302	16.5	RR
1954+513		1.220	18.5	OBC
2131+175		1.215	19.3	SSH
2150+053		1.979	17.8	Bar
2201+315	YES	0.297	15.5	NB
2248+192	YES	1.806	18.5	Bar
2305+187	YES	0.313	17.5	GH
2325+269		0.875	17.5	present
2325+293		1.015	17.3	SSH
2349+327	YES	0.659	19.9	PW
2354+144		1.810	18.2	Bar

Table 6.4 Radio jets in quasars: list of references

Bar	Barthel (1984)
dPP	de Pater & Perley (1983)
F81	Fomalont (1981)
GH	Gower & Hutchings (1984)
HUO	Hintzen <u>et al</u>. (1983)
LM	Lonsdale & Morrison (1983)
MH	Miley & Hartsuijker (1978)
NB	Neff & Brown (1984)
OBC	O'dea <u>et al</u>. (1988)
OP	Owen & Puschell (1984)
present	Chapter 3, this thesis
PW	Potash & Wardle (1980)
RR	Rusk & Rusk (1986)
S83	Saikia <u>et al</u>. (1983)
SKP	Saikia <u>et al</u>. (1986)
SKN	Schilizzi <u>et al</u>. (1982)
SBC	Stocke <u>et al</u>. (1985)
SSH	Swarup <u>et al</u>. (1984)
SSS	Swarup <u>et al</u>. (1982)
Wyck	Wyckoff <u>et al</u>. (1983)

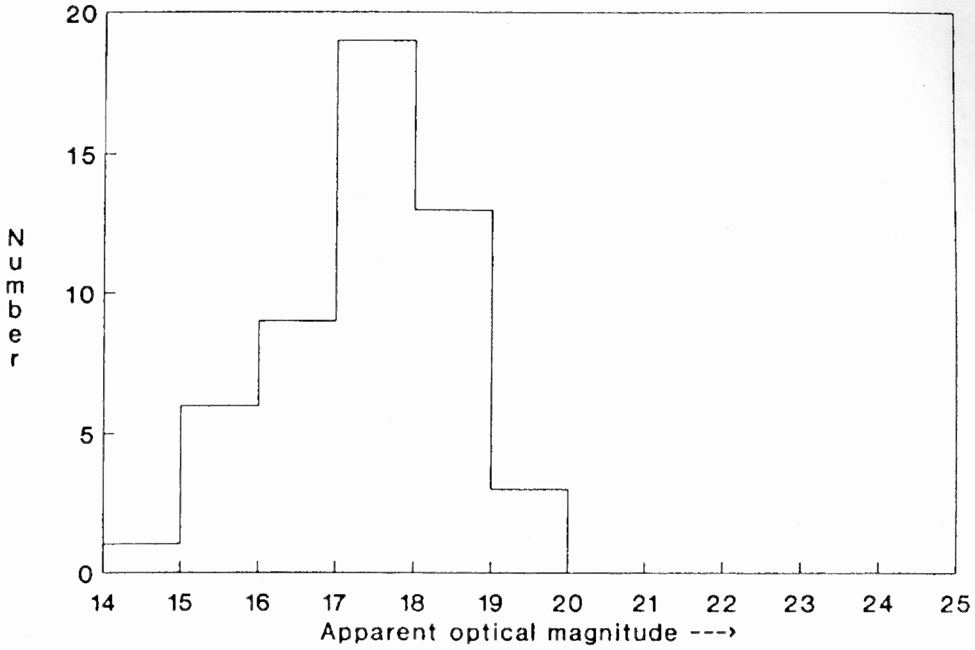

(a) Quasars with jets

Fig.6.6 Distribution of apparent optical magnitude

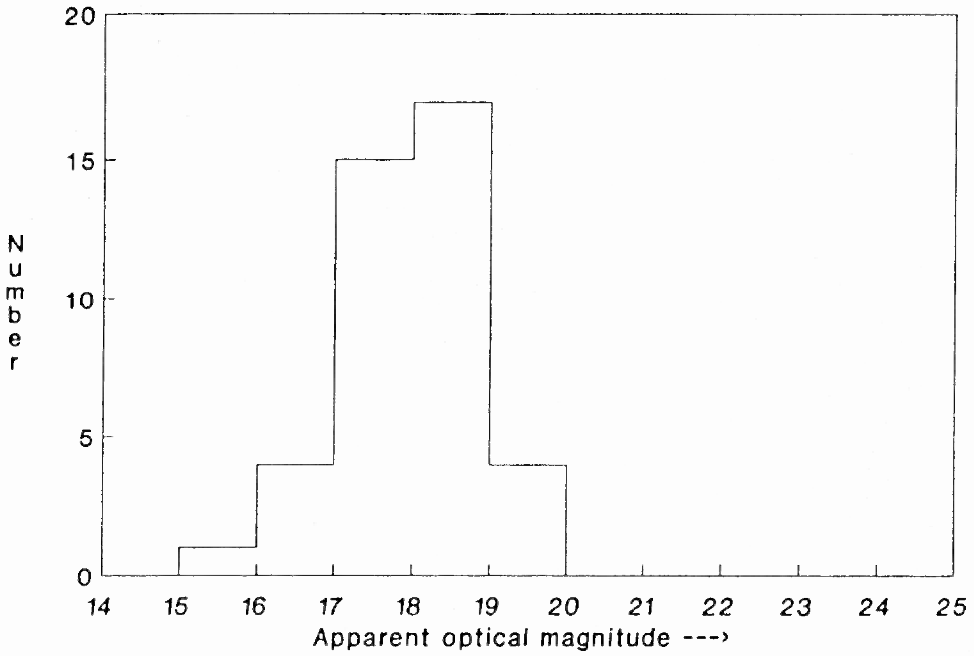

(b). Quasars without detected jets

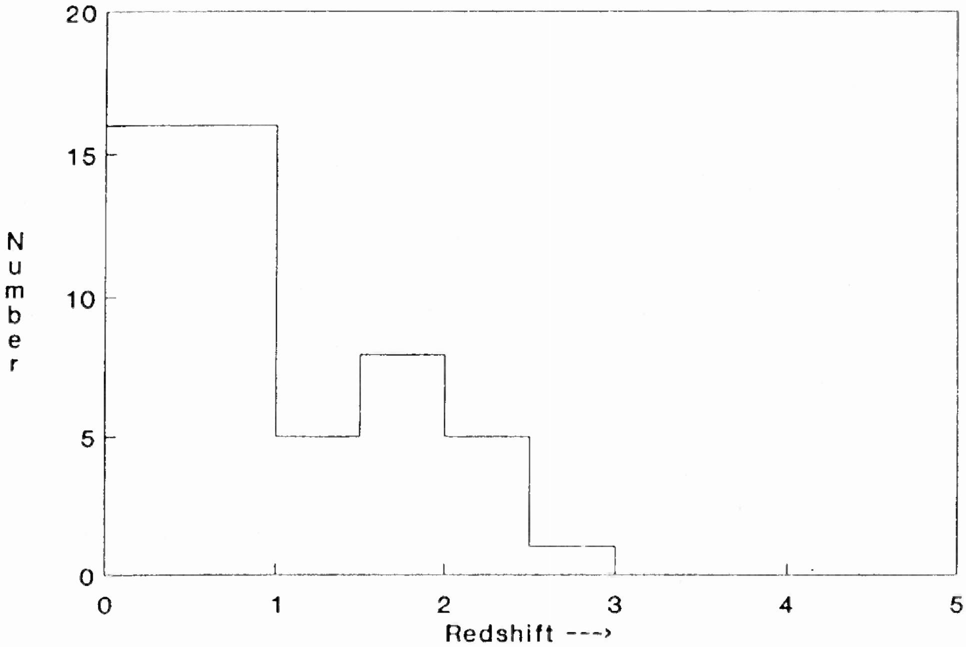

(a) Quasars with jets

Fig.6.7 Distribution of redshift

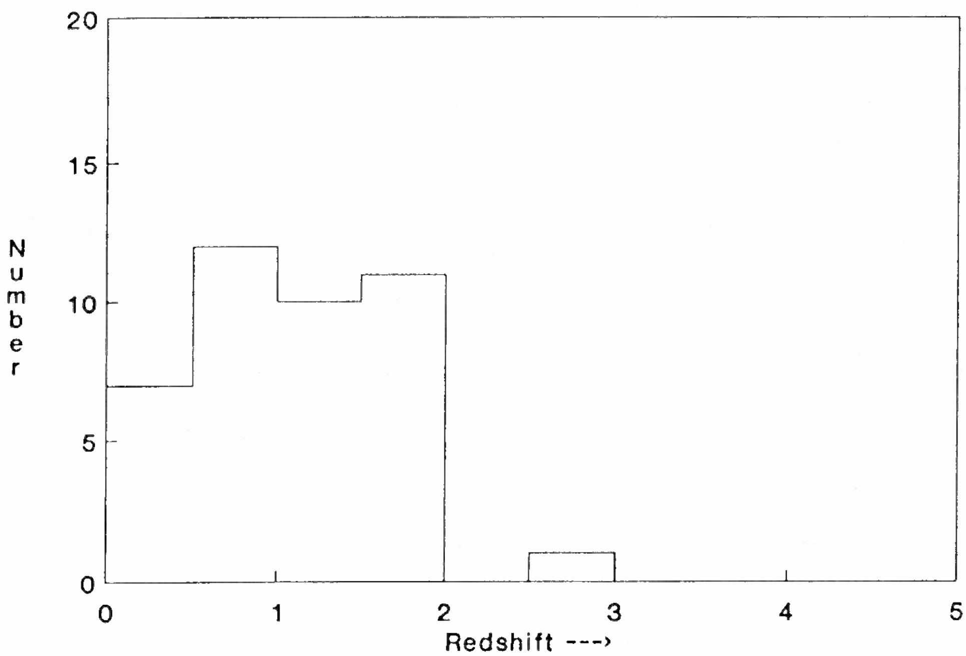

(b) Quasars without jets

relativistic motion in the nucleus, and, on the other hand, relativistic motion on a large scale also occurs. While the trend is not a very strong one, it is interesting that there is any trend at all, given that a good correlation would require alignment of structures ranging from subparsec scales to hundreds of kiloparsecs.

A possible selection effect that might lead to a spurious trend of this sort is related to the fact that surface brightness (at radio wavelengths in this case) diminishes at a very rapid rate with cosmological redshift. If the quasars that do not show the presence of a jet are also those that are at systematically higher redshifts and therefore more distant, they might also appear to have a fainter optical continuum. The redshift distributions for the two categories of quasars with and without jets (Figs. 6.7a and b) show, however, that the quasars with detected jets are not at systematically lower redshifts.

6.6 Causes of optical aspect dependence—relativistic beaming or thin disc?

Both relativistic beaming of the optical continuum (Browne & Wright, 1985) and inclination effects of an optically thick geometrically thin disc (Netzer, 1985) have been suggested as possible causes for the aspect dependence of the optical continuum. In the first case, the relativistically beamed optical and radio emission come from the same physical region, and the effect of an "optical bias" on the distribution of R should be of the same kind as that of a "radio bias" that favours orientations close to the line of sight. Since relativistic beaming effects increase steeply for small orientation angles of the radio axis with the line of sight, the orientation bias due to optical beaming (as in samples at increasingly higher frequencies) is expected to show up at the high−R end (viz., $R \gtrsim 10$) of the R-distribution (Fig. 2 in Orr & Browne, 1982). Indeed, Fig.6.1 shows an excess of quasars with large values of R. But the distribution also differs from the prediction of Orr & Browne (1982) (which was quantified using the 3CR quasars) at low to intermediate values of R (i.e., R $\lesssim$ 10), as mentioned in section 6.1.1. This suggests that the functional dependence of the optical emission on inclination angle may be very different from that of relativistically beamed radio emission.

The shift in the peak of the R-distribution relative to that predicted seems to be consistent with the "thin disc interpretation" for the optical continuum. For such a disc, the most rapid change in optical flux would be expected when the disc (and hence the radio axis) makes fairly large angles with the line of sight (because the apparent optical flux density would vary as the cosine of this angle). The consequent beaming effects at radio wavelengths are therefore expected to influence mainly the low end of the R-distribution. The data described here thus clearly indicate that the optical continuum seems to consist of at least two aspect dependent components: one that is relativistically beamed synchrotron radiation, and the other that is thermal radiation from an optically thick but geometrically thin disc.

Further, the possibility that dust around quasar nuclei may not be distributed isotropically (Netzer, 1987; Thompson *et al.*, 1988) would imply that aspect-dependent obscuration would add to the aspect-dependence of the optical continuum.

It may be added that the result of Hutchings & Gower (1985) (Section 6.4.4) does seem to imply that the radio beaming is accompanied by enhancement of the optical continuum in radio-quiet quasars also. This enhancement could be either due to relativistic beaming *or due to orientation effects of a disc* (as described in section

6.8). The latter is more likely, since given that the radio emission is itself weak, it is improbable that a large amount of jetted synchrotron emission is emitted at optical wavelengths. In fact, violent optical variability, believed to be a sign of relativistically beamed optical emission, is almost unknown radio-quiet quasars.

6.7 Implications of optical aspect dependence

It is generally implicit in investigations of the properties of quasars that the optical continuum from the nucleus is isotropic. Its possible aspect dependence, therefore, has several implications, some of which are discussed below.

6.7.1 Selection effects in low-frequency samples of radio quasars

To reiterate the assertion made in sections 6.1 and 6.2 for the Bologna quasars, *samples of quasars selected at low radio frequencies would necessarily be biased with respect to orientation unless optical identifications for the whole radio survey are complete.* Further, if a thermally emitting, opaque and thin disc is present in radio-quiet quasars also (section 6.4.4), then samples selected to be brighter than a certain apparent optical magnitude might also be biased with respect to orientation.

6.7.2 The degree of enhancement of the optical continuum

If the entire difference in the apparent magnitude distributions shown in Fig. 6.3 arises from orientation effects, the figures suggest that the enhancement of the optical continuum can typically be as high as two or three magnitudes for the Bologna quasars, somewhat larger than was suggested by Browne & Wright (1985). But it is possible that they may have underestimated the effect for the following reason. In comparing the magnitudes of CDQs and LDQs, they have *assumed* (particularly at low flux density levels) that *all* the quasars in the samples selected at 408 MHz (including the Bologna sample) are lobe-dominated. But the examples of the Bologna quasars and those from the samples of Wills & Lynds (1978) show that a substantial fraction from amongst them may turn out to be core-dominated when observed at high radio frequencies. If such (optically bright) objects are removed from the their set of LDQs selected at 408 MHz, a larger difference in the apparent magnitudes of CDQs and LDQs would result.

6.7.3 The luminosity-volume test

The luminosity-volume test (Kafka, 1967; Schmidt, 1968) is a powerful technique to statistically extract cosmological information from samples of objects whose redshifts are known. The test requires that the sample be strictly complete to some limiting flux density. (It does not require, however, that the spread in the intrinsic luminosity be narrow.) The test is applied as follows. For every object, the volume of space out to its redshift is determined in comoving coordinates in some given cosmological model. From its derived luminosity, the maximum redshift which the object could be at and still appear bright enough to be visible above the limiting flux density of the sample is computed, and thereby V_{max}, the volume of space corresponding to this cosmological distance, is calculated. If the cosmology assumed is a good approximation and if the objects in the sample are uniformly distributed in space, then it is expected that half the number of objects would be found with $V < 0.5\ V_{max}$, and the other half with $V > 0.5\ V_{max}$. The mean value of V/V_{max} for the entire sample must be 0.5. As it turns out, the exercise is not very sensitive to the exact values of H_0 and q_0 used. Thus, if $<V/V_{max}>$ exceeds 0.5, that is a demonstration that one is seeing more objects from further out.

The study by Masson & Wall (1977) of the Parkes sample of quasars selected at 2.7 GHz in the strip of sky of ± 4° declination gave a lower value of $<V/V_{max}>$ for the quasars with flat radio spectrum than for those with steep radio spectrum (0.52 ± 0.05 as opposed to 0.67 ± 0.05). The result led them to suggest that in the case of radio quasars, cosmological evolution was confined to sources with extended radio structures, while compact objects consisting only of components of high surface brightness have a uniform spatial distribution. Wills & Lynds (1978) also obtained a lower value of $<V/V_{max}>$ for flat spectrum objects than for those with steep spectrum, for complete samples of quasars selected at 178 MHz.

But the difference in the value of $<V/V_{max}>$ for quasars with flat and steep radio spectrum is entirely consistent with the difference in their respective distributions of apparent optical magnitude. If the latter is just an orientation effect as has been argued in the previous sections, then the mere fact of a lower value of $<V/V_{max}>$ is not necessarily evidence that the quasars of flat radio spectrum evolve to a lesser degree than their steep spectrum counterparts. Indeed, in the unified scheme of Orr & Browne (1982), since the quasars with flat and steep spectrum are intrinsically similar objects, one would not in general expect them to have differing evolutionary properties.

However, by the unified scheme, in a given radio flux density limited complete sample, the quasars of flat radio spectrum have a lower intrinsic luminosity than those of steep radio spectrum, because in the former case the apparent luminosity would be enhanced by Doppler boosting of the core flux density. And therefore, if there is luminosity dependent density evolution, the flat spectrum objects could show lower evolution in comparison. For instance, Peacock *et al.* (1981), using a sample of higher limiting flux density than the samples of Masson & Wall (1977) and Wills & Lynds (1978), have shown that flat radio spectrum quasars do yield a value of V/V_{max} comparable to the corresponding values for steep radio spectrum quasars in the latter samples. More recently, Morisawa & Takahara (1987) have shown that the source counts and redshift distributions of steep and flat spectrum quasars are consistent with the predictions of the unified scheme.

6.7.4 The Hubble diagram for quasars

In this section, the implications of aspect-dependence of the optical continuum for the Hubble diagram of quasars is examined.

For a homogeneous and isotropic expanding universe, assuming a value of 1 for the deceleration parameter q_0, and a value of 50 km s^{-1} Mpc^{-1} for Hubble's constant H_0,

$$\log cz = 0.2\, m_v + B,$$

where

$$B = \frac{-M_v + 5\log H_0 - 25}{5},$$

M_v is the absolute magnitude, and the unit distance is 1 Mpc.

Thus, for a given class of extragalactic objects, if it is assumed that the luminosity function is narrow, and that the measured redshift of an object is (almost) wholly of cosmological origin, the Hubble diagram, i.e., a plot of (the logarithm of) the redshift against the apparent magnitude, is expected to have a slope of 0.2. Since quasars are the most distant objects known, with the largest redshifts, the Hubble diagram of quasars is an important correlation.

The early work of Lang *et al.* (1975) showed that the Hubble plot for all of the then known quasars was compatible, within errors, with the theoretically expected value of 0.2, just as that for the normal and radio galaxies was. Of course, while almost all of the observed brightness of normal and radio galaxies in the visible wavelength region is due to their stellar emission, in quasars, it is due to the non-stellar emission from the active galactic nucleus, with thermal and non-thermal components of currently uncertain relative magnitudes.

Setti & Woltjer (1973) studied the Hubble diagram for *radio* quasars, separating them by their radio spectral index. They found that the quasars with steep spectrum showed a significant Hubble relation, though with much dispersion, and that those with flat spectrum showed an almost pure scatter diagram. The latter result, they concluded, was probably due to the broader luminosity function of the flat spectrum objects. Their result is roughly consistent with the conclusion of Netzer *et al.* (1978), viz., quasars with flat *optical* spectrum show a better Hubble correlation than those with steep *optical* spectrum. (Presumably, quasars with steep *optical* spectrum are those with flat *radio* spectrum and vice versa in the case of the radio-loud quasars (e.g., Wills & Wills, 1986). Notably though, about 50 per cent of the quasars in Netzer *et al.* (1978) were radio-quiet.)

The result of Setti & Woltjer (1973) is clearly relevant to the unified scheme, since in that framework, differences between the two classes of quasar are due to orientation effects alone. Two questions arise:

(a) Is the result of Setti & Woltjer (1973) borne out by the data that are available for the much larger number of quasars now known?

(b) If so, then can the result be understood as being due to orientation effects alone?

The answer to question (a) is in the affirmative. Fig. 6.8a and b show the Hubble plots for the radio quasars with steep and flat spectrum from the catalogue of Veron-Cetty & Veron (1987). The radio spectral indices listed in the catalogue have been used to classify the radio quasars into steep and flat spectrum categories. The V magnitudes listed in the catalogue have corrected for absorption by our Galaxy, and K-corrected, as follows:

$$m_v^{corrected} = m_v^{catalogue} - K - A_{Galaxy},$$

where, for an optical spectral index α^{opt},

$$K = -2.5\ (1+\alpha^{opt})\ \log(1+z),$$

and

$$A_{Galaxy} = \begin{cases} 0.099\ [csc(|b|)-1] & \text{for } |b|<50^\circ \\ 0 & \text{for } |b|>50^\circ \end{cases}$$

where b is the Galactic latitude (e.g., Lang *et al.*, 1975). The quasars with steep spectrum do show a better Hubble correlation than the ones with flat spectrum, a trend also reflected in the values of the least-squares fit and the absolute magnitude dispersion σ_M (listed in Table 6.5).

Question (b) can now be considered. The larger scatter in the Hubble diagram for quasars is easily understood if the relativistic beaming of the radio emission is accompanied by enhancement of the optical continuum. If a significant fraction of

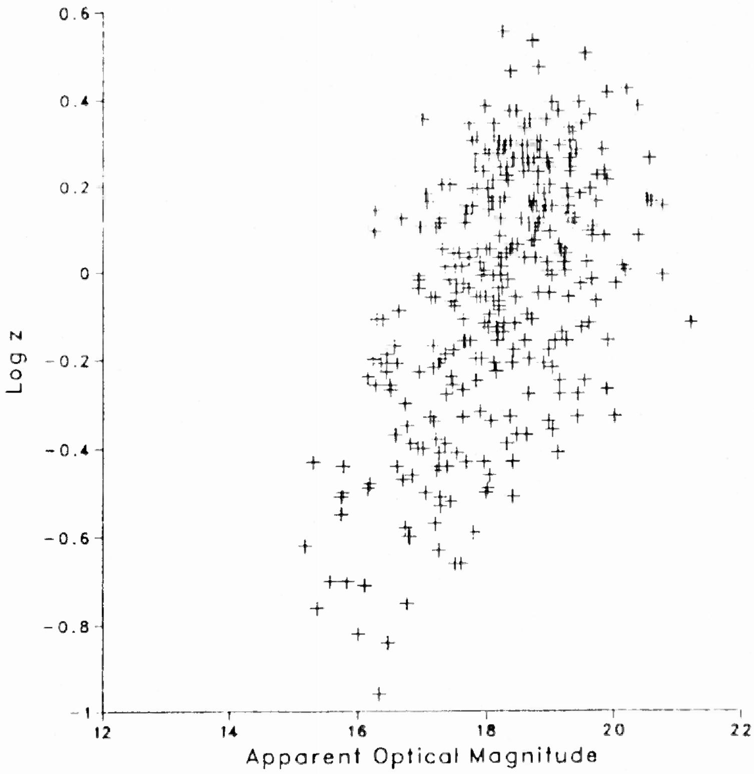

Fig. 6.8a. The Hubble Diagram
Quasars with Steep Radio Spectrum

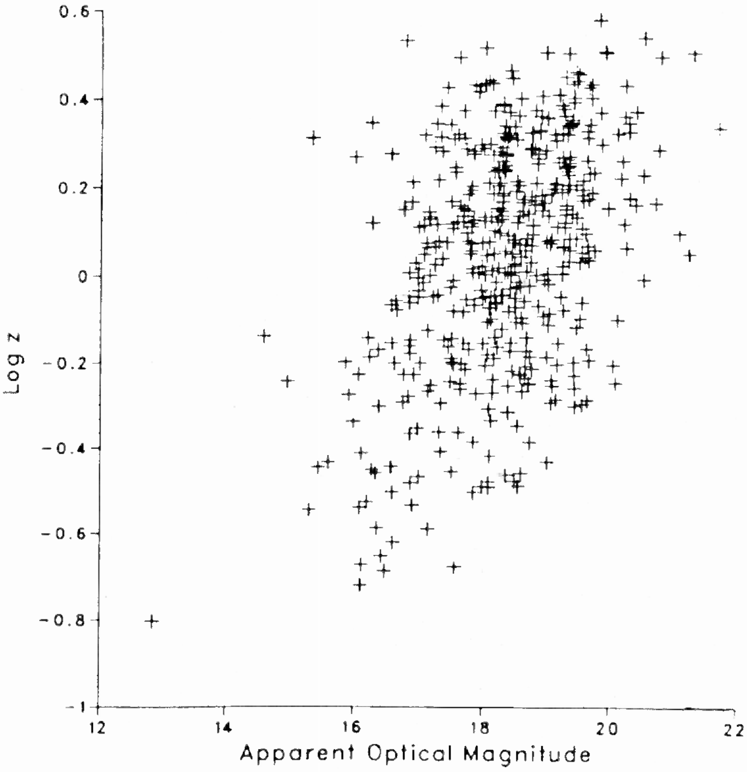

Fig. 6.8b. The Hubble Diagram
Quasars with Flat Radio Spectrum

Table 6.5 Parameters of the Hubble correlation

	Number of Objects	Slope: b	σ_b	Correlation Coeffecient (r)	Magnitude Dispersion (σ_M)
Steep Spectrum Quasars	340	0.14	0.012	0.53	1.72
Flat Spectrum Quasars	498	0.10	0.009	0.44	2.27
"Brightest" Steep Spectrum Quasars		0.23	0.037	0.85	0.85
"Brightest" Flat Spectrum Quasars		0.20	0.034	0.82	1.04

the optical emission is relativistically beamed, the luminosity function would be broadened (e.g., Urry & Shaffer, 1984), and would increase the magnitude dispersion of the Hubble diagram for the flat spectrum objects (besides the variability of the OVV quasars, which are flat radio spectrum objects). *Thus the difference in the two Hubble plots can indeed be qualitatively explained by orientation effects alone.* Further, since the aspect dependence of a thin-disc component of the optical continuum would be strongly manifest at source orientations close to the plane of the sky, it would follow that *the optical luminosity function of the steep radio spectrum sources would be broadened too,* thus contributing to scatter of the Hubble correlation.

For a set of extragalactic objects with a broad luminosity function, the brightest object at each redshift should show a tighter Hubble correlation (Bahcall & Hills, 1973; McRea, 1972). This is illustrated below. Following the procedure of Bahcall & Hills (1973), the quasars were grouped into redshift bins of 15 objects each, and M_v was calculated according to

$$M_v = m_{corrected} - 5\log z - 43.88 \ .$$

m_v^{bin} for the most luminous quasar in each bin was derived as its apparent magnitude if placed at the average bin redshift, z_{avg}. Thus,

$$m_v^{bin} = M_v^{\min} + 5\log z_{avg} + 43.88 \ .$$

The correlations are indeed better (Figs. 6.8c & 6.8d; Table 6.5).

It should be kept in mind, however, that the Hubble plots presented here are approximate for several reasons:

(a) the catalogue of Veron-Cetty & Veron (1987) is a mere compilation, not "complete" in any sense, and unknown selection effects may therefore be present;

(b) the V magnitudes used are often photographic and therefore inaccurate, and have not been corrected for the emission line luminosities;

(c) the radio spectral index is a two-point value and not necessarily derived from simultaneous measurements;

(d) a universal optical spectral index has been used to derive the K-correction (on an average, the flat radio spectrum sources would have steeper optical spectra and vice versa; therefore the use of a universal value would tend to wash out some of the difference between the two classes);

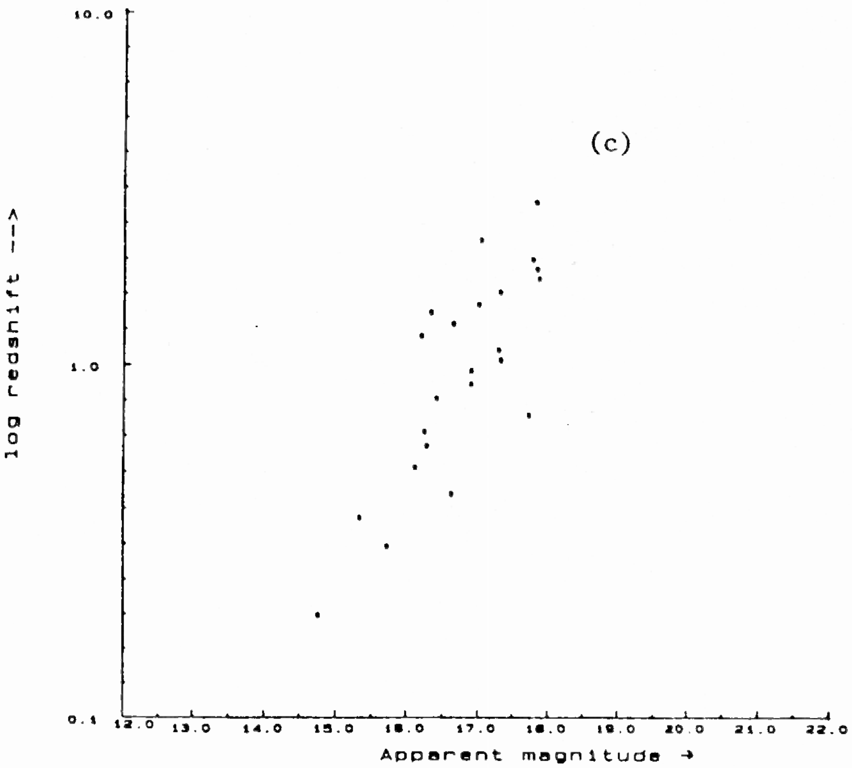

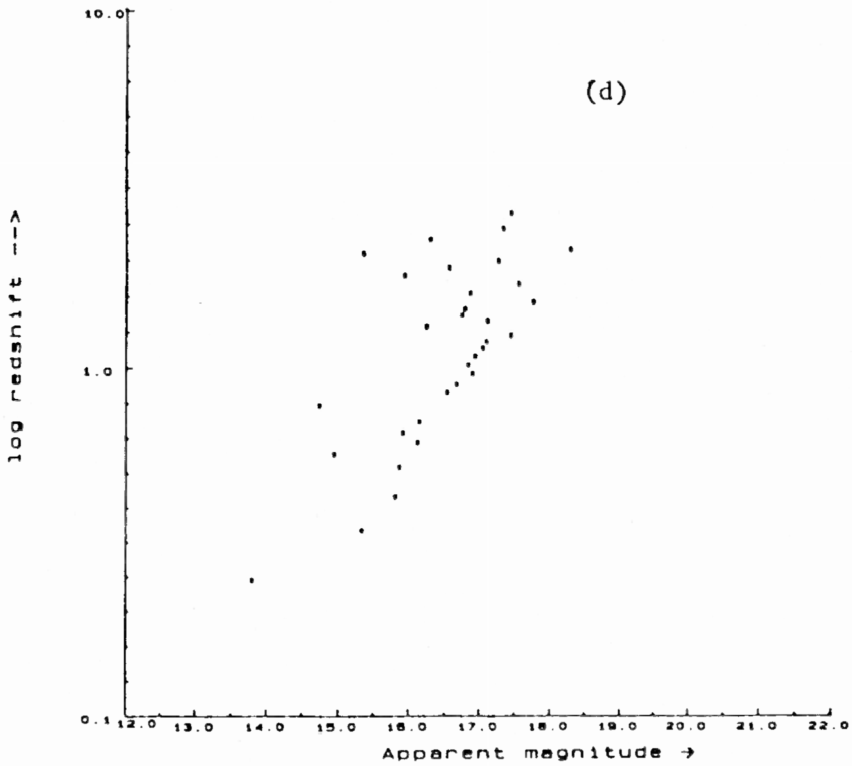

Fig. 6.8c & d. The Hubble diagram for the "brightest" steep and flat spectrum quasars respectively.

(e) the compact steep spectrum (CSS) sources should be considered separately, since they seem to belong to a different physical class, and do not partake in the unified scheme (cf. this thesis, section 4.3);

(f) the plot has not been corrected for the Malmquist bias, nor for the 'volume effect' (Kembhavi & Kulkarni, 1978).

6.7.5 The Baldwin effect

The equivalent width of the CIV emission line has been known to be inversely correlated with the luminosity of the optical continuum ("the Baldwin effect"; see, e.g., Wampler *et al.*, 1984). If a significant fraction of the optical continuum originates from an optically thick, geometrically thin disc, the Baldwin effect may immediately and naturally be explained. Netzer (1985) discusses the arguments in detail.

6.8 Summary

The apparent optical magnitudes of quasars from the Bologna sample show that if R is a statistical measure of the angle of inclination of the quasar to the line of sight, then *their optical continuum is aspect dependent*. The behaviour of the optical luminosity of the quasar nucleus to that of the host galaxy supports this proposition. There is a mild trend for large-scale radio jets to preferentially occur in optically brighter quasars, which is consistent with the suppositions that the jets are relativistically beamed and that the optical continuum is aspect dependent.

Both relativistic beaming and disc orientation effects are likely to play a significant role in causing optical aspect dependence.

Aspect dependence of the optical continuum can introduce a serious selection effect into samples of quasars selected from low-frequency surveys if all the survey objects are not optically identified. It follows that the degree of enhancement of the optical emission that is derived from comparing optical magnitudes of low- and high-frequency samples of radio quasars may be an underestimate.

Differences in the values of $<V/V_{max}>$ that obtain for flat and steep radio spectrum quasars are consistent with the corresponding differences in their optical magnitudes. If the optical continuum is aspect dependent, then the different $<V/V_{max}>$ values do not imply differing evolutionary properties for the two classes of radio quasars.

Orientation effects due to optical emission from a thin and opaque disc would increase the scatter in the Hubble diagram for quasars with steep radio spectrum, just as relativistic beaming of the optical continuum would increase the scatter in the Hubble diagram for quasars with flat radio spectrum.

While the unified interpretation of Blandford & Königl (1979) clearly cannot incorporate the radio-quiet quasars, a scheme akin to that of Scheuer & Readhead (1979) (wherein the total radio power is relativistically beamed) probably applies to them.